

Theory of defects in vitreous silicon dioxide

Eoin P. O'Reilly*

Department of Physics and Materials Research Laboratory, University of Illinois, Urbana, Illinois 61801

John Robertson

Department of Physics and Materials Research Laboratory, University of Illinois, Urbana, Illinois 61801 and Central Electricity Research Laboratories, Leatherhead, Surrey, United Kingdom

(Received 4 October 1982)

Models for defects in SiO_2 fall into the two basic categories of "vacancy-bridge" and valence-alternation models. We have calculated the local electronic structure of the main defects in each model, using the tight-binding and recursion methods. The localization of each level is found and compared to that measured by ESR for the paramagnetic centers. The silicon dangling bond, the neutral oxygen vacancy, and the positively charged oxygen vacancy (E' center) all give deep states near mid-gap. The Si-Si bond gives a bonding state in the lower gap and an antibonding state near the conduction-band minimum. The positive, threefold-coordinated oxygen site $\text{O}_3^+(\text{Si}_3)$ gives a state bound only by its Coulombic field. In general, all positively charged centers possess a "shallow" bound state 1–2 eV below the conduction-band minimum. Such shallow states account for the prevalence of optical absorption around 7.6 eV in SiO_2 . The nonbridging oxygen introduces states just above the valence-band maximum. The peroxy bridge and radical give states both at mid-gap and in the lower part of the gap. A broad absorption band around 5–6 eV is associated with the peroxy radical, for the first time. It is suggested that valence-alternation defects must still be present in $\nu\text{-SiO}_2$, but at a much lower concentration, of order 10^{15} cm^{-3} , than previously supposed, due to a higher valence-alternation creation energy in SiO_2 than in $a\text{-Se}$ or $a\text{-As}_2\text{Se}_3$.

I. INTRODUCTION

Two types of models have developed for defects in vitreous silicon dioxide, $\nu\text{-SiO}_2$. The vacancy-bridge (VB) model views SiO_2 as a wide-band-gap insulator and suggests that the oxygen vacancy and "interstitial" (as a peroxy bridge and radical) are the dominant defects.¹ The valence-alternation (VA) models regard $\nu\text{-SiO}_2$ as a chalcogenide glass like As_2Se_3 and predict the main defects to be Si and O dangling bonds and overcoordinated, positively charged oxygen sites.^{2–6} Our current knowledge is dominated by the electron-spin-resonance (ESR) active centers, which are usually associated with the VB model. We point out in this paper that some VA defects should also be present in SiO_2 , and that they must be considered for a complete understanding of its properties.

We examine the electronic structure of the main defects predicted by both models, using an empirical tight-binding scheme and the recursion method. Our results explain the absorption and luminescence transitions associated with the peroxy radical⁷ and the nonbridging oxygen-hole center.⁸ They em-

phasize that diamagnetic VA oxygen centers should be present, acting as charged scattering centers. We discuss the optical transitions associated with the paramagnetic oxygen vacancy V_{O}^+ (the E' center), and while we cannot assign all transitions, place constraints on future models. We show that with lattice relaxation significant rebonding can occur between the two Si atoms at the neutral oxygen vacancy V_{O}^0 . These Si-Si vacancy bonds could be the origin of optical transitions^{9,10} usually associated with the V_{O}^+ centers. Si-Si "wrong" bonds introduce highly localized bonding and antibonding defect levels, and should give rise to a characteristic absorption band. We argue that all positively charged defect centers possess a "shallow" state 1–2 eV below the conduction-band minimum, bound only by the Coulombic field. Transitions to these levels account for the 7.6-eV absorption band seen in a wide range of silicas.

Vitreous silicon dioxide is a wide-band-gap (~ 9 eV) network glass with directional bonding of mixed covalent and ionic character. Short-range order dominates many of its properties, with each Si and O atom being fourfold- and twofold-coordinated,

respectively, as in crystalline SiO_2 . To date, the undercoordinated silicon center¹¹⁻¹⁵ Si_3^0 , the nonbridging oxygen atom^{1,7,16,17} O_1^0 , and the peroxy radical^{7,17,18} are the only native defects which have been positively identified, all by ESR. The E' center is presumed to be a Si dangling bond at a charged oxygen vacancy V_O^+ , and has been correlated with the optical-absorption band⁹ at 5.85 eV and the luminescence band¹⁰ at 4.3 eV in $\nu\text{-SiO}_2$ (6.2 and 4.8 eV in crystalline SiO_2). The peroxy radical⁷ has been identified with the absorption peak at 7.6 eV and the O_1^0 center⁵ with absorption above 2 eV and luminescence at 1.85 eV. We explain the origins of these transitions and point to others which have not previously been identified. We argue that the 7.6-eV absorption band may arise from the neutral O vacancy V_O^0 , or positively charged centers (O_3^+ , V_O^+) rather than the peroxy radical as previously supposed.

In the next section, we review the VB and VA models. Our calculational method is described in Sec. III and the electronic structure of bulk SiO_2 in Sec. IV. Results for the oxygen and silicon centers are presented in Secs. V and VI, respectively. We discuss our results in Sec. VII and finally summarize our conclusions in Sec. VIII.

II. MODELS OF DEFECTS IN SiO_2

VB defects are generally produced by radiation displacing atoms in the network. The primary defect in the VB scheme is the oxygen vacancy (see Fig. 1). Its positive state, V_O^+ , called the E' center, contains only one electron and is paramagnetic. ESR indicates that the electron localizes preferentially onto one of the two Si dangling bonds directed into the vacancy, and that the other Si atom, now positively charged, relaxes out of the vacancy towards a planar configuration.¹¹ (This planar configuration is also found for the isoelectronic boron sites in B_2O_3 .¹⁹) Thus V_O^0 consists of one pyramidal Si_3^0 and one planar Si_3^+ . By analogy, we expect two pyramidal silicons at V_O^0 and two planar silicons at V_O^{2+} . The peroxy bridge $\equiv\text{Si}-\text{O}-\text{O}-\text{Si}\equiv$ is hypothesized to be the Frenkel counterpart of V_O as the simple oxygen interstitial is presumed to be unstable. Direct structural evidence for the bridge is difficult to find but it is the probable antecedent of the neutral peroxy radical $\equiv\text{Si}-\text{O}-\text{O}\cdot$, recently identified by ESR.^{17,18} The peroxy radical is the predominant oxygen-hole center in dry silicas (those containing less than about 10 ppm of H). In wet silicas, the nonbridging oxygen atom is the principal O center seen in ESR (Fig. 1).⁷ Its presumed antecedent is the hydroxyl radical $\equiv\text{Si}-\text{O}-\text{H}$. The properties of the VB defects and tentative assign-

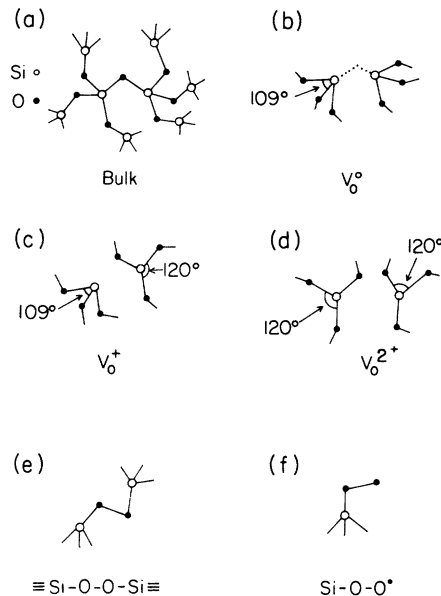
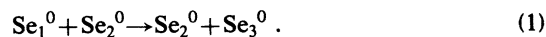


FIG. 1. Bonding configurations (a) in bulk SiO_2 , (b) at the neutral vacancy V_O^0 , (c) the positively charged vacancy V_O^+ (the E' center), (d) the doubly-charged vacancy V_O^{2+} , (e) the peroxy bridge $\equiv\text{Si}-\text{O}-\text{O}-\text{Si}\equiv$, and (f) the peroxy radical $\equiv\text{Si}-\text{O}-\text{O}\cdot$.

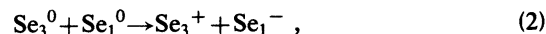
ments of their optical transitions have recently been reviewed by Griscom.¹

VA models have successfully explained such properties as the diamagnetism, Fermi-level pinning, and photoinduced luminescence and ESR in amorphous chalcogenide glasses. The VA model emphasizes the special role of the lone-pair $p\pi$ electrons at the top of the valence band.^{20,21} Like the chalcogenides, silicon dioxide has a $p\pi$ valence-band maximum. VA models have therefore been proposed to describe its defect states.²⁻⁶

VA defects are produced by breaking a $\text{Si}-\text{O}$ bond in the network.^{20,21} Undercoordinated Si_3^0 and O_1^0 paramagnetic centers are then formed (Fig. 2), with the superscript referring to the charge and the subscript to the coordination. In the chalcogenide glasses it is possible for one of the undercoordinated atoms to rebond with the lone pair from a neighboring chalcogen. This generates an extra bond in the network and an overcoordinated chalcogen site. In amorphous Se, the reaction is



In general the Se_3^0 site is less stable than the original Se_1^0 . However, it can be stabilized by the transfer of an electron from the Se_3^0 antibonding state into the dangling bond of another undercoordinated atom,



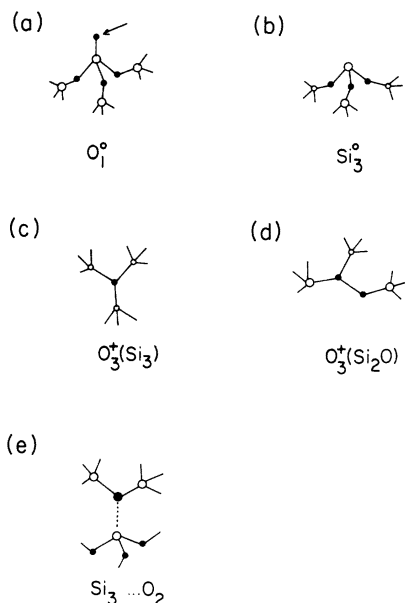


FIG. 2. Bonding configurations at (a) an isolated undercoordinated oxygen site, (b) an isolated undercoordinated Si site, (c) overcoordinated oxygen sites formed by rebonding of an Si_3^+ center as proposed by Lucovsky (Ref. 4), (d) overcoordinated oxygen site from the rebonding of O_1^+ , and (e) Si_3 interacting weakly with a normally coordinated oxygen atom, as required by the Greaves model (Ref. 3).

and we get pairs of charged diamagnetic centers in the ground state, known as valence-alternation pairs (VAP's).²¹ The transfer of the electron between the two defects and the creation of the VAP is favored if the energy gained by forming the extra bond exceeds the energy required to doubly occupy the Se_1 dangling bond. The stabilization of double occupancy compared to single occupancy in neutral defects is described as an effective negative correlation energy or "negative U ."

Two VA models have been proposed for SiO_2 . Greaves³ considered that the electronegativity difference between Si and O was sufficient to stabilize the charged centers Si_3^+ and O_1^- (Fig. 2). Lucovsky⁴⁻⁶ suggested that Si_3^+ could rebond to give an overcoordinated O_3^+ site and $O_1^- - O_3^+(Si_3)$ pairs in the network (where the parentheses indicate nearest-neighbor coordination). The rebonding of O_1^+ sites to give $Si_3^- - O_3^+(Si_2O)$ pairs is also possible, but these should be much less stable than $O_3^+(Si_3) - O_1^-$ pairs on electronegativity grounds.²²

Evidence for VA defects in ν - SiO_2 is indirect: The scattering centers of conduction electrons⁵ and the "slow" traps at the SiO_2 -Si interface could be VA centers.² The temperature dependence and Stokes shift of the 4.3-eV luminescence band are

similar to those of chalcogenide glasses.²³ Lucovsky⁴ originally attributed the peak at 606 cm^{-1} in the Raman spectrum of irradiated SiO_2 to the VA O_3^+ center. The concentration of O_3^+ centers is not high enough to explain the intensity of this line, which may instead be due to low-order rings.²⁴ We argue below that O_3^+ centers could still be present in SiO_2 , but at a lower concentration than originally proposed. The main evidence against VA centers comes from ESR data and in particular from that of the Si_3^0 center. The ^{17}O hyperfine interaction in amorphous SiO_2 indicates clearly that each Si dangling bond interacts with only three equivalent (backbonded) oxygen neighbors.¹⁵ The Greaves VA model is therefore ruled out as it requires an interaction with a fourth special oxygen atom to give the Stokes shift seen in photoluminescence. In the Lucovsky scheme this fourth oxygen is also needed as the precursor of the O_3^+ site. A comparative review of VB and VA defects in SiO_2 has recently been given by one of us²⁵ and we make further comments on the two schemes in Sec. VII.

III. METHOD

The electronic structure is calculated by taking 243-atom clusters, each consisting of 27 unit cells of α -quartz. A random structure such as the Bell and Dean amorphous-silica network²⁶ could have been considered instead but would not have significantly altered the results. Defects were embedded in the center of each network. Some, such as the oxygen vacancy, were formed by removing atoms, while others were formed by setting the tight-binding interactions between specific atoms to zero. To form undercoordinated Si and O centers, for instance, we set the direct interaction between a silicon atom and one of its four oxygen neighbors to zero. Certain defects, such as the overcoordinated oxygen center, could not be embedded in a single cluster, and were formed by joining a number of clusters together as described in Appendix A.

A s - p basis of one s and three p orbitals was used, with first-neighbor Si-O and second-neighbor O-O parameters being included (see Table I). The Si-O interactions were given values close to those of Laughlin *et al.*,²⁷ while the O-O interactions were taken from chemical pseudopotential calculations.²⁸ Second-neighbor Si-Si interactions are screened out by the oxygen atoms, and their inclusion does not improve the density of states (DOS). They were only included across the oxygen vacancy and at the Si-Si wrong bond. When bond lengths varied, the Si-O interactions were scaled as (bond length)⁻², while the second-neighbor Si-Si and O-O interactions decay exponentially with distance and were

TABLE I. Hopping interactions and orbital energies in eV.

Interaction	$-ss\sigma$	$sp\sigma$	$ps\sigma^a$	$pp\sigma$	$-pp\pi$
Si-O bulk, 1.61 Å	3.0	5.4	5.0	6.0	1.4
O-O bulk, 2.64 Å	0.15	0.35		0.56	0.13
O-O $-O_2^-$, 1.49 Å	2.80	4.15		4.5	1.45
O-O $-O_2^0$, 1.39 Å	3.60	5.15		5.4	1.80
Si-Si 2.34 Å	2.08	2.47		2.72	0.72
Si-Si 3.06 Å (unrelaxed V_O^0)	1.22	1.44		1.59	0.42
	$E(s)$	$E(p)$			
Si	4.08	10.0			
O	-1.0	-16.0			

^aSi p -O s .

calculated using the chemical pseudopotential programs.

The local DOS (LDOS) of the defect atom and its immediate neighbors were calculated using the recursion method²⁹ with each continued fraction expanded to 40 levels. Accurate information on the character of gap states was obtained using the method of "zeros and poles,"³⁰ where the LDOS is approximated by a set of δ functions, with one δ function (in the gap) being identified with the defect level.

It is necessary to modify the orbital energies of some defect and interface atoms from their bulk values to reproduce certain experimental data. The self-energies of Si orbitals in SiO₂ must be raised significantly with respect to those in bulk Si in order to fit both the gap of SiO₂ and the band discontinuities at the SiO₂:Si interface.^{25,27,31} Those of O in SiO₂ and Si in bulk Si remain close to their free-atom values. This effect is ascribed to the neglect of orbital overlap in Si-O-Si bridges, and not to Coulombic effects, as the O energies do not move. In our work, the self-energies of particular Si sp^3 hybrids are assigned values which depend on whether the hybrid faces oxygen, or another Si or is dangling, as described in Appendix B. This contrasts with the approach taken by Laughlin *et al.*²⁷ and Martinez,³¹ who, faced with similar problems, changed the energies of all the hybrids on a given Si atom, rather than just those facing Si neighbors or vacancies.

Self-energy shifts must also be included at under-coordinated oxygen sites in order to describe correctly the localization of their hole states. The shifts arise from oxygen sites attempting to remain neutral and are similar to those first noted in a -Se (see Sec. VC).³²

In summary, the self-energy changes at Si sites arise largely from the neglected orbital overlaps,

which cause individual hybrid energies to vary, while those at O sites are due to changes in orbital occupancies, which move all orbital energies at the site.

The DOS calculations of the following sections do not include the Coulombic part of the defect potential explicitly. Its effect must be added *a posteriori*. Deep states have recently been defined as those gap states which are bound only by the central-cell part of the total-defect potential.³³ Conversely, shallow states are bound by the long-range part, usually the Coulombic tail. This new definition has important consequences for SiO₂. There, the low electronic screening ($\epsilon=1.5$) causes nominally shallow states to have binding energies comparable to those for deep levels ($\sim 1-2$ eV). Shallow states can therefore be confused with true deep states if the "depth" of a trap is defined in terms of its binding energy.

Clearly shallow states need only be added *a posteriori* for charged centers. The DOS shown in the figures are those for neutral centers. The states associated with negative centers are highly localized because of the large hole mass and the major Coulombic effects are already included as on-site self-energy shifts. The states of positive centers need more careful consideration. Positive centers are not as strongly localized because of the low electron effective mass in SiO₂, and the shallow levels are bound below the conduction band by an effective Rydberg. If the central-cell potential does not bind a deep state the shallow levels are the only gap states associated with the defect. If a deep state exists, the Coulombic tail still pulls shallow levels, orthogonal to the deep levels, out of the conduction band. Hence deep positive centers like Si₃⁺ also possess additional shallow levels not included in the figures.

The binding energy of shallow levels at positive centers is essentially that of the valence exciton because of the large effective-mass ratio. This is diffi-

cult to determine experimentally in SiO_2 because of its indirect forbidden gap. The conduction-band minimum of quartz is at Γ and the valence-band maximum is at the zone boundary.³⁴ Transitions from the higher O π valence bands are forbidden in any form of SiO_2 with tetrahedral Si sites because the phases of these π orbitals prevent their coupling to Si s conduction states in the dipole approximation.³⁵ The optical spectrum of SiO_2 exhibits a large peak at 10.4 eV assigned to a direct exciton, but it is difficult to determine the onset of direct allowed band-to-band transitions and thereby estimate the exciton binding energy. Estimates of the Ryberg vary widely^{2,35}; a value of 1.5 eV is assumed here.

IV. BULK SiO_2

The calculated DOS of α -quartz is presented in Fig. 3(a) along with the experimentally measured photoemission spectra.³⁶ The two sets of spectra are in good agreement with each other. The electronic structure of SiO_2 is based on a unit made up of one oxygen atom and the two sp^3 hybrids from its silicon neighbors.³⁷ The oxygen s band is centered about -20 eV. The band between -10 and -5 eV is due to strong Si-O-Si bonding states, while the lower part of the one between -4 and 0 eV arises

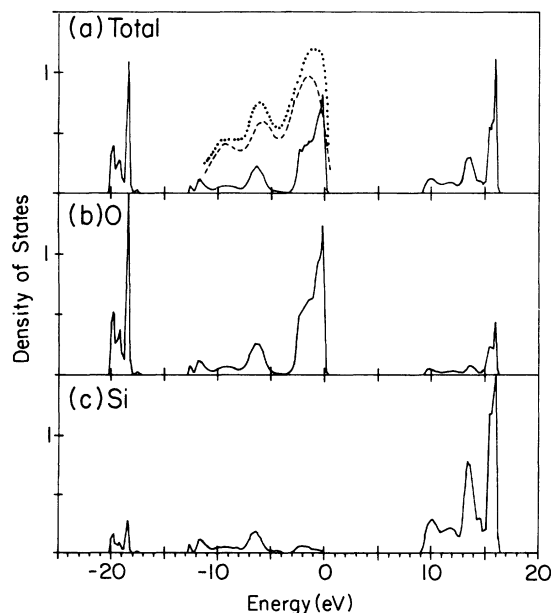


FIG. 3. (a) Calculated DOS and photoemission spectrum (Ref. 36) of SiO_2 . Fermi level lies at 0 eV. (b) and (c) are the DOS projected onto an oxygen and a silicon site, respectively. Each division on vertical scale of this and following diagrams indicates 0.5 electrons $\text{eV}^{-1}\text{atom}^{-1}$.

from Si-O-Si weak-bonding states. The top of the valence band, just below 0 eV, comes from oxygen lone-pair $p\pi$ orbitals. These $p\pi$ states will play an important role in many of the defects considered below.

Figures 3(b) and 3(c) show the DOS projected onto an oxygen and a silicon site, respectively. The valence bands project mainly onto the oxygen site. There is a net charge of $+2.3e$ on each silicon and $-1.15e$ on each oxygen, indicating an ionicity of about 60%. The calculated band gap is 9.0 eV as compared with the experimental value of 8.9 eV.^{2,35,38}

V. OXYGEN CENTERS

A. Nonbridging oxygen

The calculated LDOS at the nonbridging (or onefold-coordinated) oxygen atom is shown in Fig. 4(a). The isolated Si-O bonding state is weaker than the strong Si-O-Si bonding state, so the band between -10 and -5 eV is replaced by a Si-O bonding peak at -4.4 eV. The two $p\pi$ orbitals, which are perpendicular to the bond, give rise to the lone-pair peak at -1 eV. Because of the reduced coordination the oxygen s state lies at -17.8 eV, above the corresponding bulk band.

Filling the valence band in Fig. 4(a) gives the negatively charged O_1^- center, while the O_1^0 center is

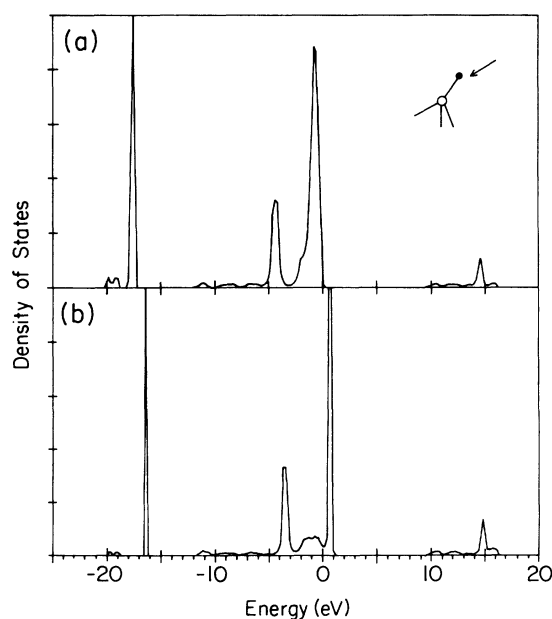


FIG. 4. LDOS at an undercoordinated oxygen atom (nonbridging oxygen center) assuming (a) no orbital energy shift and (b) all orbitals on undercoordinated oxygen site raised by 1.5 eV due to charge-transfer effects.

formed by creating a hole in this band. For the O_1^- center, charge-transfer effects raise the self-energies of the oxygen orbitals and lift the $p\pi$ states into the gap. Self-energy shifts also occur at the O_1^0 center. Figure 4(a) indicates that the $p\pi$ orbitals couple to $p\pi$ orbitals on neighboring oxygen sites, forming the lone-pair band of width 1.5 eV. The hole formed by creating O_1^0 would then be quite delocalized, leaving a significant negative charge on the onefold-coordinated site. This raises orbital energies on the O_1^0 site until they are consistent with the local charge transfer. In Fig. 4(b) we show the LDOS at the O_1^0 site with the orbital energies raised by 1.5 eV. (This is consistent with the self-energy shift at the peroxy radical.) Two $p\pi$ lone-pair states rise above the valence-band edge, giving a highly localized hole state at 0.62 eV. This state has 92% of its weight on the oxygen $p\pi$ orbital, as in ESR, where the nonbridging oxygen hole center is found to be essentially 100% localized in one oxygen p orbital.⁷

The O_1^- center also gives gap states. Being negatively charged, its self-energies and gap states are shifted even higher than those for O_1^0 .

A number of localized transitions involving the gap states are possible [see Fig. 5(a)]. Electrons can

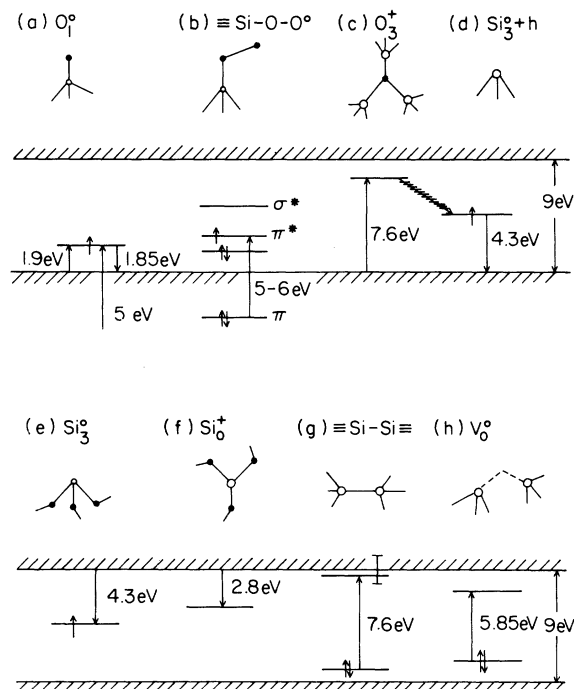


FIG. 5. Proposed optical transitions due to defects in SiO_2 : (a) excitations at nonbridging oxygens, (b) excitations at peroxy radicals, (c) excitation of an electron into the shallow state of O_3^+ , followed by its relaxation to (d) Si_3^0 and recombination with 4.3-eV luminescence, (e) and (f) other transitions at Si_3^0 and Si_3^+ , (g) $\sigma \rightarrow \sigma^*$ transition at a Si-Si bond, and (h) possible transitions at V_0^0 .

be excited from the valence band into the hole state of O_1^0 . The transition is localized on the Si-O bond and so in an exact calculation its energy should be calculated by transition-state methods. A 1.85-eV luminescence band, correlated with nonbridging oxygen centers,⁸ could arise from recombination of electrons in the gap state with holes in the valence band. Little bond relaxation is expected at the nonbridging oxygen center, so that there should only be a small Stokes shift. The 1.85-eV band can be excited by light of energy between 1.9 eV and over 5 eV. At the lower end of the excitation spectrum, electrons are lifted from the valence-band maximum to the defect state, while at the upper end, they come from deeper in the band, with the hole left behind then becoming localized at the band edge. The nonbridging oxygen level in silicate glasses is also believed to lie above the valence-band maximum of SiO_2 and causes much of the 2.5-eV reduction in their optical gap.^{2,39,40}

B. Peroxy bridge

We calculate the electronic structure of the peroxy bridge assuming the same atomic configuration as in H_2O_2 , where the O-O bond length is 1.49 Å and the two O-H bonds have a relative dihedral angle of 100° .⁴¹ The DOS projected onto one of the bridging oxygens is shown in Fig. 6. The O-O bond dominates the LDOS. It gives rise to a bonding $p\sigma$ resonance at -4.4 eV and an empty $p\sigma^*$ gap state at 4.2 eV. The oxygen $2s$ band splits into a pair of states at -23.2 and -15.5 eV. Of the two p orbitals not directly involved in the O-O bond, one forms a bond with the neighboring Si atom, while the other is essentially a $p\pi$ lone-pair orbital. The $p\pi$ orbital is almost parallel to the O-Si bond of the neighboring oxygen atom. The O-Si bonding state lies predominantly on the oxygen site and interacts with the $p\pi$ orbital to raise it just out of the lone-pair band and 0.35 eV into the gap. This gap state

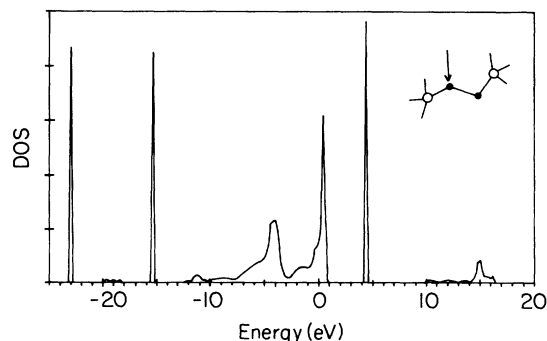


FIG. 6. LDOS of an oxygen atom in a peroxy bridge $\equiv Si-O-O-Si \equiv$.

is filled in the neutral peroxy bridge, and is thus ESR inactive. Because of its localization on an O lone-pair orbital, direct transitions from this state to the bottom of the conduction band are forbidden [see Fig. 5(b)]. An allowed transition should occur between the oxygen $p\sigma$ bonding band at -4.4 eV and the empty $p\sigma^*$ state at 4.2 eV, giving an absorption band near 8.6 eV.

C. Peroxyl radical

The peroxy radical has the same atomic and electronic configuration as the undercoordinated Se center ($-\text{Se}-\text{Se}'$) in amorphous Se, with a onefold-coordinated chalcogen being bonded to a normally coordinated one in each. Vanderbilt and Joannopoulos³² found that with this configuration a unique lone-pair interaction, described below, causes a significant charge transfer between the two terminal atoms, raising the orbital self-energies on the defect site. In Se the self-energies are raised by 1.25 eV, while we find that in SiO_2 they must be raised by 2.0 eV to obtain the peroxy-hole localization seen in ESR.¹⁸

The electronic structure of the radical is calculated including the 2.0 -eV self-energy shift on the terminal site and assuming the same atomic configuration as in the $\text{H}-\text{O}-\text{O}'$ radical, with the $\text{O}-\text{O}$ bond length set to 1.39 Å and the $\text{Si}-\text{O}-\text{O}$ bond angle set to 106° (Fig. 7).⁴² The oxygen $2s$ levels split into a bonding-antibonding pair, as in the bridge, and the $\text{O}-\text{O}$ bond again produces a $p\sigma$ resonance, now at -3.6 eV, and an empty $p\sigma^*$ gap state at 6.6 eV. The antibonding states lie predominantly on the terminal site [Fig. 7(a)] due to the self-energy shifts. Of the two $p\pi$ orbitals on the terminal oxygen, one gives the filled lone-pair state at 1.8 eV, while the other lies parallel to and interacts with the lone-pair orbital on the next-to-last oxygen, giving a $p\pi$ bonding resonance at -2.4 eV and a half-filled $p\pi^*$ state 2.1 eV above the valence-band edge.

This terminal π interaction causes the charge transfer between the two sites and consequent increase in the defect-site self-energy. The next-to-last atom contributes two electrons from its lone-pair orbital and the terminal atom contributes one to the $p\pi$ - $p\pi^*$ pair. If both atoms had the same orbital energies, they would share these three electrons equally, causing a net transfer of 0.5 electrons to the terminal atom. To compensate this charge transfer, the Coulomb interaction raises the orbital energies on the onefold-coordinated atom,³² thereby increasing its share of the $p\pi^*$ hole. The $p\pi^*$ state is half-filled in the neutral peroxy radical and is found from ESR to have 75% of its weight on the terminal site and 25% on the next-to-last one.¹⁸ Our self-

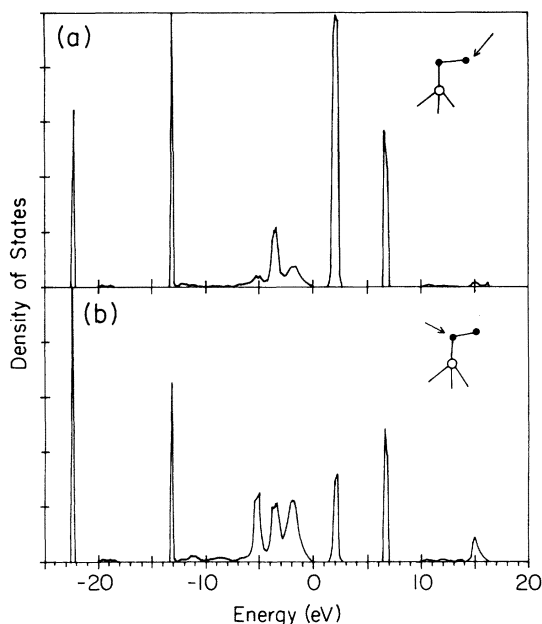


FIG. 7. LDOS at a peroxy radical $\equiv\text{Si}-\text{O}-\text{O}'$ projected onto (a) the terminal oxygen site and (b) the next-to-last one. With the use of the zeros and poles method (Ref. 30), two states are resolved under the broad peak in the lower half of the gap, at 1.8 and 2.1 eV, respectively.

energy shift was chosen to fit this experimentally determined wave function.

Two allowed transitions in particular should occur at the radical in Fig. 5(b): one between the lone-pair $p\pi$ and $p\pi^*$ states and another between the $p\sigma$ and $p\sigma^*$ states. The $p\pi$ resonance and the half-filled $p\pi^*$ state are split by 4.5 eV in our calculations. In gaseous $\text{H}-\text{O}-\text{O}'$, a broad absorption band at 6 eV is due to transitions between these two states.⁴³ Introducing O_2^- into NaCl gives an absorption band at 5 eV due to oxygen $p\pi$ - $p\pi^*$ transitions.⁴⁴ Our calculations may underestimate the $p\pi$ - $p\pi^*$ transition energy, as is common in chemical pseudopotential calculations. We therefore expect an absorption band at 5 – 6 eV in SiO_2 . This has not been identified yet, probably because of its overlap with stronger bands, in particular, the 5.85 -eV band associated with the E' center. Support for this argument comes from the annealing studies of Friebele *et al.*¹⁶ They found that the correlation between the annealing of the ESR intensity of the E' center and the 5.85 -eV band is best in samples of wet silica, where the predominant oxygen defect is the non-bridging oxygen center. In dry silicas, where the peroxy radical dominates, significant absorption occurs at 5 – 6 eV after annealing the E' center. We attribute this absorption to the $p\pi$ - $p\pi^*$ transition.

The 7.6 -eV absorption band which has been corre-

lated with the peroxy radical⁷ cannot be due to the oxygen $p\sigma$ - $p\sigma^*$ transition. We find a splitting of over 10 eV between these levels, so the associated absorption should lie above the band gap. Furthermore, the peroxy bridge is the presumed antecedent of the radical and, because of the greater atomic separation, the O—O bond is weaker there than at the radical. Therefore, if the 7.6-eV band arises from σ - σ^* transitions at the radical, a lower-energy peak of similar width and intensity should be associated with the bridge. No evidence has been found for such a band.

D. $O_3(Si_3)$

The overcoordinated oxygen site $O_3^+(Si_3)$ is the most important oxygen defect in the VA defect scheme. It is isoelectronic with the N site in Si_3N_4 , which is planar or near-planar. A pyramidal structure is, however, also possible, as is more commonly found for threefold-coordinated group-V atoms (e.g., NH_3). The DOS with the Si-O-Si angle set equal to both 120° (planar) and 98° have been calculated and are presented in Fig. 8. The Si—O bond length has

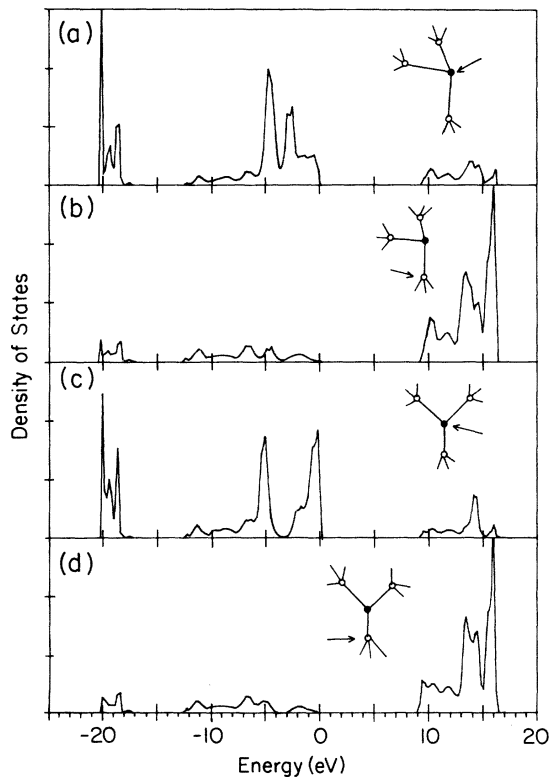


FIG. 8. (a) LDOS at an overcoordinated oxygen site, and (b) at one of its three silicon neighbors assuming a pyramidal bonding configuration. (c) and (d): the same for planar bonding.

been increased from the bulk value of 1.61 to 1.71 Å, because of the threefold coordination, as suggested by Lucovsky.⁶

For both the C_{3v} pyramidal [Figs. 8(a) and 8(b)] and the D_{3h} planar structures [Figs. 8(c) and 8(d)], the Si—O bonds remove all states from the gap, leaving a resonance at the bottom of the conduction band. A net charge of $-0.8e$ is found on O_3^+ in our calculations and $+2.25e$ on each of the neighboring silicons, leaving the center with an overall $+1e$ charge compared to the bulk. The Coulombic tail of the O_3^+ center produces a shallow state at 7.4–8 eV, as discussed in Sec. III. Owing to the threefold coordination, a resonance occurs at the bottom of the oxygen s band. The chief difference between the pyramidal and planar oxygen LDOS is in the lone-pair, weak-bonding band at -4 to 0 eV. With pyramidal bonding, much of the weight in this band is shifted towards lower energies, whereas with planar bonding a p lone-pair resonance is found just below the valence-band edge. This defect is only expected to be stable in the charged state O_3^+ . Upon capture of an electron, it reconstructs by breaking an Si—O bond to give an Si_3 center.

E. $O_3(Si_2O)$

The last oxygen center that we consider is the $O_3^+(Si_2O)$ site, formed by overcoordination of an O_1^+ site. This defect is the amphoteric partner of Si_3^- in the VA scheme.²² Its electronic properties are dominated by the O—O bond (Fig. 9). We assume that the threefold-coordinated oxygen [Fig. 9(a)] is in a pyramidal configuration. The characteristic oxygen $2s$ structure is seen around -20 eV. An empty $p\sigma^*$ antibonding state is found below midgap, whose exact energy depends on the O—O bond length. A sharp resonance at the top of the valence band is localized chiefly on the $O_2(SiO)$ site and arises mainly from its lone-pair orbital. In the planar-bonding configuration, the filled lone-pair orbitals on the two oxygen atoms would interact to give a $p\pi$ bonding resonance in the valence band and a fully occupied $p\pi^*$ antibonding state above the band edge. Inclusion of the Coulomb potential would pull a defect state out of the conduction band, giving a shallow level near 7.4 eV.

VI. SILICON CENTERS

A. Silicon dangling bond

The isolated undercoordinated silicon atom Si_3 is the most important silicon-related defect in the VA scheme. We examine the pyramidal neutral state Si_3^0 and the planar charged center Si_3^+ . We set the self-energy of the sp^3 dangling bond in Si_3^0 and p -

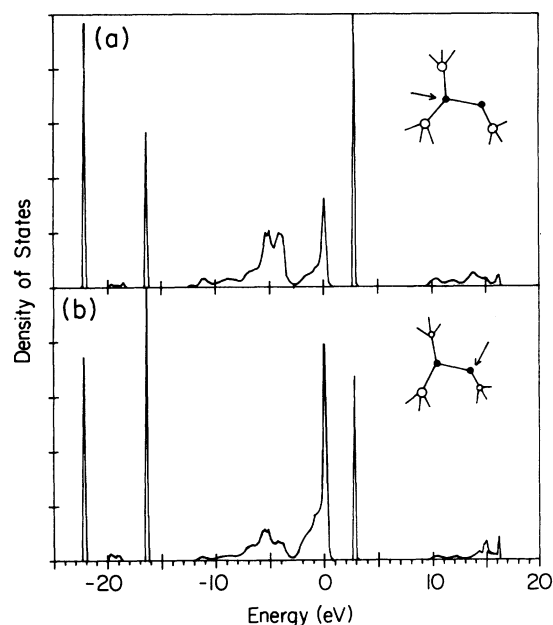


FIG. 9. (a) LDOS of an oxygen atom bonded to two silicon neighbors and one oxygen neighbor. (b) The LDOS at the oxygen neighbor.

like dangling bond in Si_3^+ to the bulk silicon value, 4 eV below that of the other hybrids (see Appendix B).

The LDOS at an unrelaxed Si_3^0 site is presented in Fig. 10(a). A highly localized gap state is found at

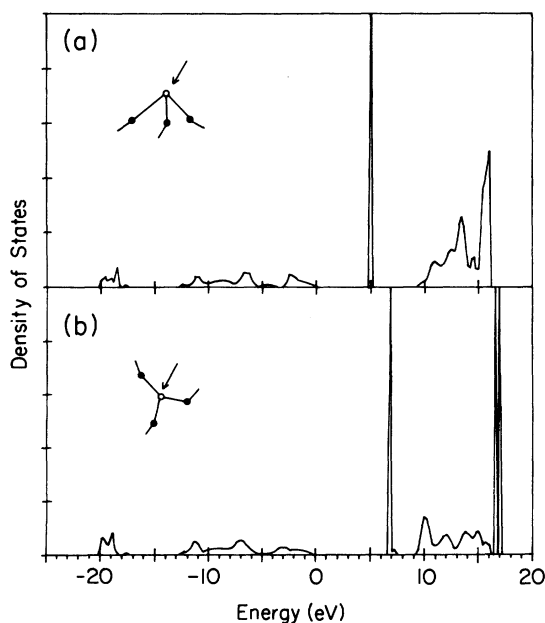


FIG. 10. (a) LDOS at an isolated pyramidally bonded Si_3^0 site. (b) LDOS at an isolated planar bonded Si_3^+ site.

4.9 eV, or 0.4 eV above the sp^3 hybrid energy and close to the valence-band edge of bulk silicon. This state has 32% s character and 52% p character at the defect site. Otherwise, the LDOS is virtually unchanged from that of a bulk Si atom in SiO_2 .

We assume that the Si_3^+ site relaxes to the planar configuration without any other movement of the lattice, so the Si—O bonds are slightly shorter than at the pyramidal site. A sharp $p\pi$ -like dangling-bond state is found at 6.7 eV, or 0.7 eV above the Si p energy [Fig. 10(b)], which is 88% localized on the p orbital perpendicular to the bonds to the three nearest neighbors. This state would move downwards if an additional Coulombic self-energy shift were included. Two σ^* antibonding Si—O states are found at 15 eV which are of e symmetry. A resonance of a_1 symmetry is found at the bottom of the conduction band. This again is a σ^* state and so lies within the Si—O bonding plane. The Coulombic potential transforms this resonance into a shallow state at about 7.4 eV. Thus we believe there are two states associated with Si_3^+ , a deep π and a shallow σ^* state.

The extremely high localization of both the Si_3^0 and Si_3^+ states causes their energies to follow closely the input hybrid energies. Our predictions therefore are clearly model dependent. If the hybrid energies are shifted less, say, in proportion to the number of backbonded oxygens, then Si_3 and the related vacancy levels (see below) will be placed higher in the gap. We have largely ignored correlation at these centers. The Coulombic repulsion will be largely intra-atomic at Si_3^- and Si_3^+ and so could shift the on-site self-energies and hence the energies of the defect levels at these centers.

B. Oxygen vacancy

The oxygen vacancy is best considered in terms of its two-component Si_3 sites. In the neutral vacancy V_{O}^0 two pyramidal Si_3^0 centers interact, giving a weak Si—Si bond. The separation of the two Si atoms at an unrelaxed vacancy is 3.06 Å, only 30% greater than the Si—Si distance in bulk Si. ESR indicates that the electron at the positive vacancy V_{O}^+ localizes preferentially on one of the Si atoms, giving Si_3^0 and Si_3^+ sites. Si_3^0 retains its pyramidal bond angles, while Si_3^+ relaxes towards the planar configuration described above. We expect the doubly-charged vacancy V_{O}^{2+} to consist of two planar Si_3^+ sites.

The electronic structure of the unrelaxed neutral vacancy V_{O}^0 is presented in Fig. 11. Two sp^3 hybrids interact to give a filled σ and an empty σ^* state. These levels are placed at 3.0 and 7.0 eV using

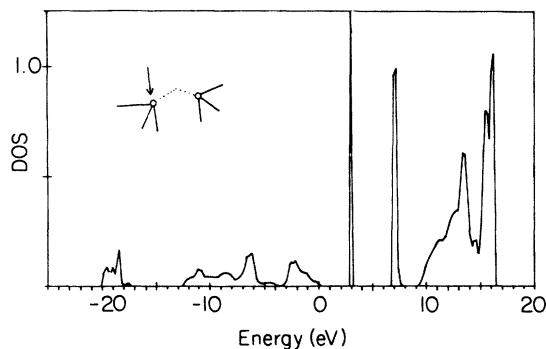


FIG. 11. DOS projected onto one of the two Si_3 sites at the neutral oxygen vacancy V_{O}^0 . No lattice relaxation is assumed.

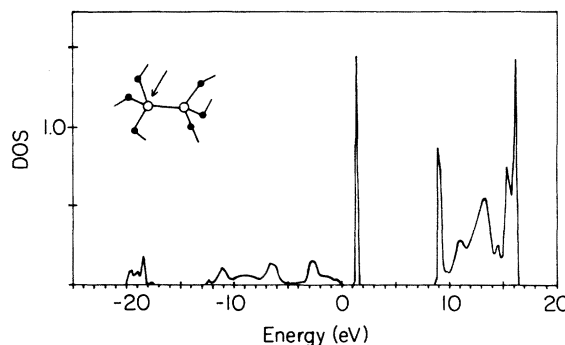


FIG. 12. DOS projected onto one of the two silicon atoms in a Si-Si wrong bond.

interactions calculated by chemical pseudopotential methods.²⁸ This assumes the hybrids are unmodified by the surrounding network and probably overestimates the σ - σ^* splitting at the unrelaxed vacancy.

The observed splitting in a real vacancy will be highly dependent on the degree of relaxation of the surrounding lattice. The mean coordination of SiO_2 is sufficiently low that the Si-Si distance could vary over a wide range, even in quartz. The strength of this bond can be optimized while maintaining approximately tetrahedral bond angles without imposing a large strain on the lattice. Given even moderate reconstruction, a clearly defined Si-Si bond should therefore exist at V_{O}^0 .

Turning to V_{O}^+ , the preferential localization of its single electron on one of the vacancy Si sites¹¹⁻¹⁵ indicates that the two Si atoms interact very weakly with each other at this center. Thus, experimentally, the defect levels and wave functions associated with V_{O}^+ should be very close to those of isolated Si_3^0 and Si_3^+ centers. We therefore expect a half-filled dangling-bond state close to 4.9 eV and an empty p -like dangling bond at or below 6.7 eV. Being positively charged, V_{O}^+ also possesses a shallow state at 7.4 eV, as did Si_3^+ . We also expect that V_{O}^{2+} , where the Si atoms are even further apart, is very similar to two isolated Si_3^+ centers, with two almost degenerate empty dangling states near 6.7 eV. The gap states and resonances have similar orbital character to those in their parent Si_3 centers.

C. Si-Si bond

The electronic structure of the Si-Si wrong bond is presented in Fig. 12. Such defects are expected in oxygen-deficient samples of SiO_2 . Two silicon sp^3 hybrids interact to give a filled strong-bonding σ state at 1.2 eV and an empty σ^* level at 8.9 eV.

The splitting between the σ and σ^* states is 7.7 eV in our calculations. While we have confidence in our calculated splitting, the mean value of the σ - σ^* states, i.e., the Si hybrid energy, may lie higher. Our present results position both the σ and σ^* states within the band gap, whereas a higher value of the Si hybrid energy would place the σ^* state within the conduction band. The σ - σ^* optical transition should give a distinct band near the intrinsic absorption edge at 7.6 eV.

VII. DISCUSSION

A. General

To date most native defects identified in SiO_2 have been of the VB type. There is little evidence for VA defects. In this section we consider the extent this reflects the experimental techniques employed and the type of samples studied or whether it requires abandoning the VA model for SiO_2 . The VB centers have been identified chiefly via ESR measurements. As ESR only probes paramagnetic defects, it can give no direct information concerning the presence or absence of diamagnetic VA centers. Secondly, most of the samples studied have in some way been removed from the vitreous SiO_2 ground state, either by γ -irradiation, neutron bombardment, or the fiber-drawing process. These processes may introduce new defects into the material, different from the preexisting ground-state defects.

It is essential to know whether incident radiation merely excites preexisting defects or creates further defects. The VB defects seen by ESR are generally observed in highly γ -irradiated quartz or v - SiO_2 samples. New centers are almost certainly being created in concentrations of order 10^{17} cm^{-3} . γ rays and neutrons are sufficiently energetic to knock on atoms, rather than just breaking individual bonds, and so create oxygen vacancies, peroxy bridges, etc.

Less energetic photons create electron-hole pairs and ionize (break) individual bonds. VA defects are of the broken-bond type.

ESR data for the E' center in γ -irradiated SiO_2 appear to refute the VA model for Si centers.¹⁵ No special neighboring oxygen atom is seen, as required in the Lucovsky and Greaves models. Also an isolated Si_3 dangling bond should have an axially symmetric g tensor, as seen at E' centers at the SiO_2 surface.⁴⁵ The g tensor of a bulk E' center has orthorhombic symmetry even in $\nu\text{-SiO}_2$, indicating an ordered environment for the Si_3^0 , as in the vacancy.¹⁴ Recently, however, further E' -like centers have been discovered in x -irradiated $\nu\text{-SiO}_2$.⁴⁶ These anneal out below room temperature and may have axial g tensors, and as such, could be related to VA defects.

In spite of this evidence, there are problems in abandoning completely the VA model for SiO_2 . The bonding in SiO_2 is covalent so breaking a single bond to create a VA defect pair should require less energy than breaking two bonds to create an oxygen vacancy. Thus VA defects should be thermodynamically preferred to vacancies. Otherwise, one is forced to postulate that VA defects attract each other and pair up into VB centers, perhaps because some screening process has lowered the energy of V_O .

A resolution to these difficulties is to propose that VA defects are indeed the intrinsic defects in unirradiated and, perhaps, strained SiO_2 while γ rays produce VB centers. The VB defects then mask the effects of the lower density of VA defects in ESR experiments.

The expected density of VA centers can be derived from their creation energy. It is generally supposed that a density of VAP's characteristic of the glass transition temperature T_g is frozen into the glass on cooling.^{21,23} In $\alpha\text{-Se}$ a VAP creation energy of 0.3 eV with $T_g = 330$ K gives a density of about 10^{19} defects per cubic centimeter. We suggest a density of about 10^{15} cm^{-3} of VAP's in SiO_2 corresponding to a VAP creation energy of 2.6 eV with $T_g = 1350$ K. Compared with their respective band gaps, the creation energy is proportionately larger in SiO_2 . This may be due to the poorer screening at O_1^- in SiO_2 and the $\text{Si} \cdots \text{Si}$ repulsions which cause $\text{O}_3(\text{Si}_3)$ to be planar.²²

This interpretation requires the 4.3-eV luminescence band to be associated with both isolated Si_3 and E' centers. A 4.3-eV band, excited by 7.6-eV light and associated with the E' center,^{10,23} is also seen in unirradiated $\nu\text{-SiO}_2$. If the intrinsic defects in SiO_2 are of the VA type, Si_3 must also give excitation and luminescence bands at these energies. We shall show that this is so in the next section.

The $\text{O}_3^+(\text{Si}_3)$ is the stable positive VA defect in $\nu\text{-SiO}_2$, not Si_3^+ . Although originally incorrectly associated with the 606-cm^{-1} Raman line of $\nu\text{-SiO}_2$ and thus supposed to be present in unrealistically large quantities, a density of, say, 10^{15} cm^{-3} of these centers would be tenable. Glass scientists generally associate valences of only 1 or 2 with oxygen in silicated glasses. O_3^+ are, however, the only oxygen sites in the covalent crystal Zn_2SiO_4 and in other phenacites.¹⁹ Zn appears to be tetravalent in silicate glasses,⁴⁷ implying the presence of O_3^+ there as well.⁴⁸

More native defects must exist in SiO_2 than have so far been identified by ESR. The E' center, the peroxy radical, and the nonbridging oxygen radical are all believed to be trapped hole centers.⁴⁶ As radiation creates electron-hole pairs, trapped-electron centers should also exist for compensation.

O_3^+ may be one of the "missing" electron traps in the VB scheme. We have argued that an independent O_3^+ is chemically more stable than Si_3^+ .²² It is diamagnetic and is not easy to identify experimentally. On capture of an electron, it forms an Si_3^0 site, which may be only metastable at room temperature.

B. Optical transitions

To date few firm correlations have been made between optical transitions and particular defect states in SiO_2 . This contrasts with the situation in other systems, where optical data often play a major role in defect identification. Most defect-absorption bands in SiO_2 are studied in irradiated samples and luminescence usually involves the decay of defects in an excited state. The photoinduced luminescence found by Gee and Kastner²³ is an important exception, as it involves transitions at preexisting defects. Further understanding of defects in SiO_2 now requires the laborious process of correlating the intensities of the various transitions with the concentrations of particular ESR centers. We must also examine the role of diamagnetic centers, for instance, through annealing studies or photoinduced ESR measurements.

Figure 5 shows the major subgap optical transitions seen in SiO_2 . We attempt to assign the various bands to specific transitions. Our assignments for the silicon centers are less firmly grounded than those for the oxygen centers, but place constraints on future models of these centers. It is noticeable that transitions at 7.6 eV could have a number of assignments. This energy occurs so frequently for two reasons. It corresponds to the excitation energy to shallow states of any positive center. Secondly, transitions from localized oxygen states at the bot-

tom of the gap to the conduction-band minimum are no longer forbidden, and some lie in this range.

A luminescence band at 1.85 eV has been correlated with the nonbridging oxygen center.⁸ This can be excited by light between 1.9 eV (Ref. 8) and over 5 eV.³⁹ We suggest excitation involves transitions from the valence band to the O_1^0 gap state [Fig. 5(a)]. The hole left in the valence band becomes a trapped polaron at the valence-band maximum. The luminescence is then due to electron-hole recombination.

No sub-band-gap absorption is expected at the peroxy bridge $\equiv\text{Si}-\text{O}-\text{O}-\text{Si}\equiv$. For the peroxy radical, we identify for the first time a broad absorption band at 5–6 eV due to transitions localized at the O–O bond between its $p\pi$ valence-band resonance and its half-filled $p\pi^*$ gap state [Fig. 5(b)]. The same transition gives a band at 5 eV for O_2^- in NaCl (Ref. 44) and at 6 eV for the free $\text{H}-\text{O}-\text{O}^{\cdot}$ radical in a vacuum.⁴³ An absorption band at 7.6 eV has been correlated via ESR with the peroxy radical.⁷ We argue that this band is probably due to transitions at a diamagnetic center formed along with $\text{Si}-\text{O}-\text{O}^{\cdot}$. If, however, it arises from transitions at the radical itself, it is most likely due to an excitation from the $p\pi^*$ gap state to an upper conduction band.

Various transitions have been experimentally correlated with the presence of silicon centers. The 4.3-eV luminescence and the 5.85-eV absorption correlate with E' centers.^{1,9,49,50} The 4.3-eV luminescence is excited by 7.6-eV photons²³ but presently absorption at this energy has been correlated with peroxy centers.¹ The origin of the 2.8-eV luminescence band¹⁰ is unknown. Our assignments for these transitions depend on which center is presumed to be present, V_O , O_3^+ , or $\equiv\text{Si}-\text{Si}\equiv$. This applies particularly to the 4.3-eV luminescence whose excitation and luminescence spectra depend strongly on the sample type.²³ Both spectra are sharp and strong in neutron-irradiated quartz, with excitation at 7.6 eV and emission at 4.8 eV. Emission in ν - SiO_2 is at lower energy, 4.3 eV. In unirradiated samples the absorption and emission are weak with a sharp excitation spectrum but a broad emission spectrum. In irradiated samples the effects are stronger, the emission spectrum sharpens up, and the excitation spectrum develops a low-energy shoulder.

The simplest assignment is for unirradiated ν - SiO_2 where we argued that O_3^+ was the dominant center. In our model in Figs. 5(c) and 5(d), a valence electron is excited by 7.6-eV photons into the shallow O_3^+ level. The center then relaxes nonradiatively in classic VA fashion²¹ into a Si_3^0 center. The hole is likely to be trapped nearby as a polaron, and

can recombine with the electron giving 4.3-eV luminescence. The broadness of the emission line may reflect the variation of the transition energy with electron-hole separation. This could be confirmed experimentally by time-resolved luminescence.

Transitions at V_O are more difficult to assign because of its complexity and the unknown relaxation in some of its charge states. In our calculations V_O^+ possesses deep states around 5 and 6.7 eV and a shallow state at around 7.4 eV. We argue that V_O^+ is the only stable configuration to possess the Si_3^+ site, as elsewhere independent sites rebond to give O_3^+ . V_O^+ has similarities to O_3^+ . Valence electrons can be excited to its shallow level by 7.6-eV photons. If the center then relaxes without forming a weak Si–Si bond, the electron and hole will recombine with emission at 4.3 eV. A number of other transitions are possible, such as those illustrated in Figs. 5(e) and 5(f). The 2.8-eV luminescence corresponds to the calculated position of the deep level on the flat Si_3^+ at V_O^+ .

Two Si sp^3 hybrids interact at Si–Si wrong bonds to give σ and σ^* states split by 7.7 eV in our calculations. Thus the Si–Si bond also produces characteristic absorption around 7.6 eV. We find both states in the gap but the σ^* level may in fact be a conduction-band resonance. If so, $\sigma \rightarrow \sigma^*$ transitions [Fig. 5(g)] might also give 4.3-eV luminescence. The excited electron enters the σ^* resonance. The Si–Si bond, now containing only one electron, relaxes to give either an isolated Si_3^0 center or a much weakened Si–Si bond. The electron then decays back into the gap state emitting light around 4.3 eV.

At V_O^0 , two Si sp^3 hybrids interact to form a weak bond, giving a σ and σ^* state in the gap. The splitting between the two states is highly dependent on the degree of relaxation and assumed strength across the vacancy, but, in any case, a clearly defined bond is formed. Some characteristic absorption band is expected due to $\sigma \rightarrow \sigma^*$ transitions at V_O^0 [Fig. 5(h)]. We assign the 5.85-eV absorption band commonly seen in SiO_2 (Ref. 9) to this transition. Both the σ and σ^* states should lie in the gap. Upon exciting an electron into the σ^* state, the bond would become unstable, and the center relaxes outward until the σ and σ^* levels are almost degenerate. The excited electron then returns nonradiatively into the σ -bonding level. Such a picture is consistent with the absence of any photocurrent or photoluminescence associated with the 5.85-eV band.¹

C. Electron scattering

Holes form polarons in ν - SiO_2 but electrons, remarkably, behave as free carriers thanks to a low ef-

fective mass and the absence of a mobility edge in the conduction band. The scattering frequency determines the electron mobility and is given by

$$1/\tau = N\sigma v,$$

where N is the density of scattering centers, σ their effective cross section, and v the electron velocity. Lucovsky⁵ attributed the scattering to a high density, of order $3 \times 10^{19} \text{ cm}^{-3}$, of defects, which per force must then be either paired or dipolar, with a small scattering cross section. We suggest a much lower concentration of defects which can now be separate, Coulombic scatterers of higher cross section as in Refs. 2 and 3.

VIII. CONCLUSIONS

Models for defects in SiO_2 fall into the two broad categories of VB and VA models. The defects in γ -irradiated and fiber-drawn SiO_2 are of the displaced-atom VB type with little evidence of VA defects. There remains, however, the possibility that defects in unirradiated vitreous SiO_2 may be of the broken-bond VA type.

The characteristic absorption bands could be due to any of these centers. For the nonbridging oxygen, a highly localized state is found above the valence-band edge. We assign the optical-absorption band at 2 eV in SiO_2 to excitation of electrons into this state giving the O_1^- center. The trapped electrons then decay back into the valence band, giving a narrow luminescence band at 1.85 eV and little Stokes shift.⁸

The DOS of the peroxy bridge and radical have many features in common and are dominated by the O—O bond. The peroxy bridge cannot be detected directly by ESR or sub-band-gap optical absorption.

Self-energy shifts localize the peroxy hole state predominantly on the terminal atom of the radical. A broad optical-absorption band at 5–6 eV is identified for the first time as arising from lone-pair $p\pi$ - $p\pi^*$ transitions at the radical. An optical-absorption band at 7.6 eV (Ref. 5) could be due to excitation from the radical $p\pi^*$ state but is more likely due to transitions at other centers.

Absorption at 7.6 eV can occur at a number of defects. Shallow levels, associated with positively charged defects, such as O_3^+ or Si_3^+ , will lie 1–2 eV below the conduction-band edge, or about 7.6 eV above the valence band. Si—Si wrong bonds give σ and σ^* gap states split in our calculations by 7.7 eV.

$\text{O}_3^+(\text{Si}_2\text{O})$ is expected to be unstable on electronegativity grounds. $\text{O}_3^+(\text{Si}_3)$ is a stable configuration in Zn_2SiO_4 and Be_2SiO_4 and is argued to be also present in SiO_2 , acting as an electron scattering center. It is a diamagnetic center, and so has no as-

sociated ESR signal. $\text{O}_3^+(\text{Si}_3)$ gives a state 1–2 eV below the conduction-band edge, localized only by its Coulomb potential. Transitions to this state could give the 7.6-eV-photoluminescence excitation band associated with the E' center. The center then relaxes giving $\text{O}_2(\text{Si}_2)$ and Si_3^0 . The luminescence is due to the electron in Si_3^0 recombining with the valence-band hole.

Both the Si_3^0 and Si_3^+ centers give highly localized states near midgap, lying near the isolated sp^3 and p hybrid energies, respectively. The 5.85-eV band correlated with the E' center cannot then be due to transitions between the Si_3^0 and Si_3^+ levels as previously supposed. We assign it instead to transitions at the neutral oxygen vacancy V_{O}^0 . With lattice relaxation, significant rebonding occurs at V_{O}^0 and the two Si_3^0 interact to give a σ - σ^* pair in the gap. Transitions between these two states give no photocurrent or luminescence, as is also found with the 5.85-eV band.

We suggest that further experiments should be carried out which distinguish between existing defects and newly created ones. In particular, defects created by γ rays should be reexcited by less energetic photons. Photoinduced ESR measurements, with sub-band-gap photons, would indicate the concentration of diamagnetic centers in the ground state and more clearly assign particular absorption bands to specific transitions. They could indicate for dry silicas whether annealing proceeds via the creation and annihilation of defect centers or, as is more likely, via charge transfer between existing centers. Time-resolved luminescence would give information on the charge state of radiative centers. The study of oxygen-deficient silicas⁵¹ and SiO_x prepared by sputtering would also be fruitful, particularly in the crossover region from Si—Si bonds to supposed oxygen vacancies.

At present, there are many gaps in our understanding of the intrinsic defect centers in vitreous SiO_2 . Measurements such as those proposed here would go a long way towards improving our understanding and towards finally answering to what extent, if at all, valence-alternation defects occur and are the native defects in SiO_2 .

ACKNOWLEDGMENTS

We have benefited greatly from discussions with D. L. Griscom, W. B. Fowler, O. K. Sankey, and J. D. Dow. We gratefully acknowledge the support of the U. S. Army Research Office (Grant No. ARO-DAAG29-81-K-0069) (for the work of J.R.), and the U. S. Department of Energy, Division of Materials Sciences under Contract No. DE-AC02-ER011198.

APPENDIX A: THE OVERLAPPING CLUSTER METHOD

The overlapping cluster method is a technique for calculating the electronic structure of defects in amorphous materials. Its advantage lies chiefly in its application to defect complexes and overcoordinated defects, as will be illustrated below. We demonstrate the method with the threefold-coordinated lattice shown in Fig. 13(a). To create a twofold-coordinated defect in this lattice, we can simply set the interaction between the central atom (site 1) and one of its neighbors (site 2) equal to zero [Fig. 13(b)]. The shortest path between the two defects so created passes through four atoms, so their mutual interaction should be negligible. For a fourfold-coordinated defect, we take a second cluster in which we have created a twofold-coordinated defect, and join it to the first through the two undercoordinated central atoms, as shown in Fig. 13(c). We then calculate the electronic structure of this bridging atom. No interactions are allowed between the atoms in the two overlapping clusters except at this bridging site.

For SiO_2 , an oxygen atom was removed from the center of a 243-atom cluster of α -quartz, leaving two silicon dangling bonds pointing into the vacancy so created. The direct interaction between the two silicon atoms is set to zero. Defect centers can then

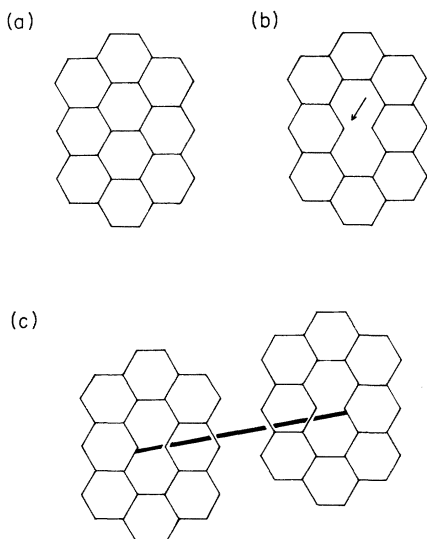


FIG. 13. (a) A defect-free threefold-coordinated lattice. (b) A pair of twofold-coordinated defects produced by breaking a bond in a threefold-coordinated lattice. (c) A fourfold-coordinated defect in a threefold-coordinated structure created by joining undercoordinated sites from two different lattices. The two sites joined by the heavy line are treated as being the same atom.

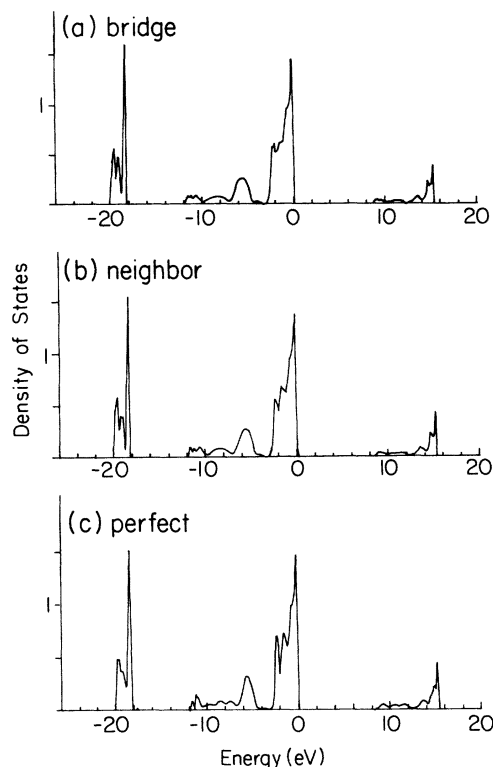


FIG. 14. LDOS on oxygen atom at (a) bridging site between two clusters, (b) on one of the neighboring oxygen sites, and (c) at core of a perfect 243-atom cluster.

be created by using one of the Si dangling bonds as a bridge between clusters.

To illustrate the accuracy of the technique, a perfectly coordinated SiO_2 structure was formed by joining two 242-atom clusters of α -quartz together via a bridging oxygen atom. In Fig. 14(a), we present the LDOS on this bridging atom. The LDOS on one of the neighboring oxygen sites is presented in Fig. 14(b) and that of an oxygen atom at the center of a normal 243-atom cluster in Fig. 14(c). The three figures are practically identical. Not only do the bands in all three have the same widths but also most of the features resolved in the perfect-cluster DOS are also resolved in the model-cluster LDOS's, where very little redistribution of spectral weight occurs. The results for Si sites, though not presented here, are equally satisfying.

APPENDIX B: Si ORBITAL ENERGIES IN SiO_2

The orbital self-energies of Si atoms in SiO_2 must be raised significantly with respect to those in bulk Si to fit the gap of SiO_2 and the band discontinuities at the SiO_2 :Si interface. Following Laughlin *et al.*²⁷ we attribute this to the neglect of orbital overlap in

empirical tight-binding calculations. We use orbitals whose energies are directionally dependent, with sp^3 hybrids which point towards oxygen neighbors being given the bulk SiO_2 energy ϵ , and those which point towards Si neighbors or into a vacancy being given the bulk Si energy $\epsilon + 4\Delta$ ($\Delta < 0$). In an sp^3 hybrid basis, the on-site interaction matrix for a Si atom with one Si and three oxygen neighbors becomes

$$\begin{pmatrix} \epsilon + 4\Delta & V & V & V \\ V & \epsilon & V & V \\ V & V & \epsilon & V \\ V & V & V & \epsilon \end{pmatrix}, \quad (\text{B1})$$

where V is the usual intra-atomic matrix element between sp^3 orbitals. As we work in an s - p basis of one s and three p orbitals, we must transform (B1) to that basis. With the Si neighbor along the (l, m, n)

direction, (B1) becomes

$$\begin{pmatrix} \epsilon_s + \Delta & L\Delta & M\Delta & N\Delta \\ L\Delta & \epsilon_p + L^2\Delta & LM\Delta & LN\Delta \\ M\Delta & LM\Delta & \epsilon_p + M^2\Delta & MN\Delta \\ N\Delta & LN\Delta & MN\Delta & \epsilon_p + N^2\Delta \end{pmatrix}, \quad (\text{B2})$$

where $(L, M, N) = \sqrt{3}(l, m, n)$. sp^3 orbitals whose energies are directionally dependent are represented in an s - p basis by the inclusion of off-diagonal elements in the self-energy matrix. Similar matrices can be formed for Si atoms with one and two oxygen neighbors.

We set the Si self-energies in bulk silicon 4 eV below those in bulk SiO_2 . The bottom of the Si conduction band is then 3.5 eV below that of SiO_2 , as found experimentally at the SiO_2 :Si interface.³⁵

*Present address: School of Physical Sciences, National Institute of Higher Education, Ballymun Dublin 9, Ireland.

¹D. L. Griscom, Proc. Freq. Cont. Symp. **37**, 98 (1979); D. L. Griscom, in *Physics of SiO_2 and its Interfaces*, edited by S. T. Pantelides (Pergamon, New York, 1978), p. 232; D. L. Griscom, J. Non-Cryst. Solids **40**, 211 (1980).

²N. F. Mott, Adv. Phys. **26**, 363 (1977); J. Non-Cryst. Solids **40**, 1 (1980).

³G. N. Greaves, Philos. Mag. B **37**, 447 (1978); J. Non-Cryst. Solids **32**, 295 (1979).

⁴G. Lucovsky, Philos. Mag. **39**, 513 (1979); **41**, 457 (1980).

⁵G. Lucovsky, Philos. Mag. B **39**, 531 (1979).

⁶G. Lucovsky, J. Non-Cryst. Solids **35-36**, 825 (1980).

⁷M. Stapelbroek, D. L. Griscom, E. J. Friebele, and G. H. Sigel, J. Non-Cryst. Solids **32**, 313 (1979).

⁸G. H. Sigel and M. J. Marrone, J. Non-Cryst. Solids **45**, 235 (1981).

⁹R. A. Weeks and E. Sonder, in *Paramagnetic Resonance*, edited by W. Low (Academic, New York, 1963), Vol. 2, p. 869.

¹⁰C. E. Jones and D. Embree, J. Appl. Phys. **47**, 5365 (1976).

¹¹F. J. Fiegel, W. B. Fowler, and K. L. Yip, Solid State Commun. **14**, 225 (1974); K. L. Yip and W. B. Fowler, Phys. Rev. B **11**, 2327 (1975).

¹²R. A. Weeks, Phys. Rev. **130**, 570 (1963).

¹³D. L. Griscom, E. J. Friebele, and G. H. Sigel, Solid State Commun. **15**, 479 (1974).

¹⁴D. L. Griscom, Phys. Rev. B **20**, 1823 (1979).

¹⁵D. L. Griscom, Phys. Rev. B **22**, 4192 (1980).

¹⁶E. J. Friebele, D. L. Griscom, and G. H. Sigel, in *Non-*

Crystalline Solids, edited by G. H. Frischat (Trans Tech, Aedermannsdorf, 1977), p. 154.

¹⁷D. L. Griscom and E. J. Friebele, Phys. Rev. B **24**, 4896 (1981).

¹⁸E. J. Friebele, D. L. Griscom, M. Stapelbroek, and R. A. Weeks, Phys. Rev. Lett. **42**, 15 (1979); **42**, 46 (1979).

¹⁹R. W. G. Wyckoff, *Crystal Structures* (Wiley, New York, 1963).

²⁰R. A. Street and N. F. Mott, Phys. Rev. Lett. **35**, 1293 (2075); N. F. Mott, E. A. Davis, and R. A. Street, Philos. Mag. **32**, 961 (1975); N. F. Mott, J. Phys. C **13**, 5433 (1981).

²¹M. Kastner, D. Adler, and H. Fritzsche, Phys. Rev. Lett. **37**, 1504 (1976); M. Kastner and H. Fritzsche, Philos. Mag. B **37**, 199 (1978); **37**, 285 (1978); H. Fritzsche, J. Phys. Soc. Jpn. **49**, Suppl. A, 39 (1980).

²²J. Robertson, Philos. Mag. B **41**, 661 (1980).

²³C. M. Gee and M. Kastner, Phys. Rev. Lett. **42**, 1765 (1979); J. Non-Cryst. Solids **35-36**, 927 (1980); **40**, 577 (1980).

²⁴F. L. Galeener, J. Non-Cryst. Solids **49**, 53 (1982).

²⁵J. Robertson, Phys. Chem. Glasses **23**, 1 (1982).

²⁶R. J. Bell and P. Dean, Philos. Mag. **25**, 1381 (1972).

²⁷D. J. Chadi, R. B. Laughlin, and J. D. Joannopoulos, in *Physics of SiO_2 and its Interfaces*, Ref. 1, p. 55; R. B. Laughlin, J. D. Joannopoulos, and D. J. Chadi, Phys. Rev. B **20**, 5528 (1979); **21**, 5733 (1980).

²⁸D. W. Bullett, J. Phys. C **8**, 2695 (1975).

²⁹R. Haydock, V. Heine, and M. J. Kelly, J. Phys. C **5**, 2845 (1972); **8**, 2591 (1975); V. Heine, in *Solid State Physics*, edited by H. Ehrenreich, F. Seitz, and D. Turnbull (Academic, New York, 1980), Vol. 35, p. 1; R. Haydock, *ibid.*, p. 215.

³⁰With the recursion method the Green's function is ex-

panded as a continued fraction, terminated after 40 levels here. The continued fraction can be written as a sum over poles, giving

$$G(E) = \sum w_i / (E - E_i) .$$

The LDOS, which is $1/\pi$ times the imaginary part of G , is then approximated by a set of δ functions, each of weight w_i and energy E_i . The weight and energy of one δ function within the band gap converge towards those of the appropriate defect state.

- ³¹E. Martinez and F. Ynduráin, *Phys. Rev. B* **24**, 5718 (1981).
- ³²D. Vanderbilt and J. D. Joannopoulos, *Phys. Rev. Lett.* **42**, 1012 (1979); *Phys. Rev. B* **22**, 2927 (1980).
- ³³H. J. Hjalmarson, P. Vogl, D. J. Welford, and J. D. Dow, *Phys. Rev. Lett.* **44**, 810 (1980).
- ³⁴J. R. Chelikowsky and M. Schlüter, *Phys. Rev. B* **15**, 4020 (1977).
- ³⁵R. B. Laughlin, *Phys. Rev. B* **22**, 3021 (1980).
- ³⁶T. H. DiStefano and D. E. Eastman, *Phys. Rev. Lett.* **27**, 1560 (1971); H. Ibach and J. E. Rowe, *Phys. Rev. B* **10**, 710 (1974); B. Fisher, R. A. Pollak, T. H. DiStefano, and W. D. Grobman, *ibid.* **15**, 3193 (1977).
- ³⁷S. T. Pantelides and W. A. Harrison, *Phys. Rev. B* **13**, 2267 (1976).
- ³⁸T. H. DiStefano and D. E. Eastman, *Solid State Commun.* **9**, 2259 (1971). T. H. DiStefano, in *Physics of SiO₂ and its Interfaces*, Ref. 1, p. 382.
- ³⁹G. H. Sigel, *J. Non-Cryst. Solids* **13**, 392 (1973/74).
- ⁴⁰S. R. Nagel, J. Tauc, and B. G. Bagley, *Solid State Commun.* **20**, 245 (1976).
- ⁴¹R. L. Redington, W. B. Olson, and P. C. Cross, *J. Chem. Phys.* **36**, 1311 (1962).
- ⁴²R. J. Blint and M. D. Newton, *J. Chem. Phys.* **59**, 6220 (1973).
- ⁴³C. J. Hochenadel, J. A. Ghormley, and P. J. Ogren, *J. Chem. Phys.* **56**, 4426 (1972); S. R. Langhoff and R. L. Jaffe, *ibid.* **71**, 1475 (1979).
- ⁴⁴J. Rolfe, *J. Chem. Phys.* **70**, 2463 (1978).
- ⁴⁵G. Hochstrasser and J. F. Antonini, *Surf. Sci.* **32**, 644 (1972).
- ⁴⁶D. L. Griscom and E. J. Friebele, *Radiat. Eff.* (in press).
- ⁴⁷R. Pettifer, *Trends in Physics* (European Physical Society, York, 1978).
- ⁴⁸J. Robertson, *Philos. Mag.* **B 41**, 177 (1980).
- ⁴⁹D. L. Griscom and W. B. Fowler, in *Physics of MNOS Devices*, edited by G. Lucovsky, F. Galeener, and S. T. Pantelides (Pergamon, New York, 1970), p. 97.
- ⁵⁰O. F. Schirmer, in *Physics of MNOS Devices*, Ref. 49, p. 102.
- ⁵¹E. Holzenkampfer, F. W. Richter, J. Stuke, and U. Voget-Grote, *J. Non-Cryst. Solids* **32**, 337 (1979).